Domain theory for capillary condensation hysteresis

Benoit Coasne,[1,*] Keith E. Gubbins,[1] and Roland J.-M. Pellenq[2]
[1]*Department of Chemical and Biomolecular Engineering, North Carolina State University, 113 Riddick Labs, Raleigh, North Carolina 27695-7905, USA*
[2]*Centre de Recherche en Matière Condensée et Nanosciences, Campus de Luminy, Case 913, 13288 Marseille Cedex 09, France*
(Received 6 February 2005; revised manuscript received 3 June 2005; published 25 July 2005)

We discuss how the original domain theory for capillary condensation hysteresis [D. H. Everett, *The Solid–Gas Interface*, Vol. 2 (Marcel Dekker, New York, 1967), pp. 1055–1113] must be modified to account for the presence of the film adsorbed at the pore surface. We show that the original predictions (scanning behavior, congruence) are not valid unless the existence of the adsorbed film is neglected or the dependence of its thickness on the pressure is neglected. We also calculate the scanning curves and subloops that are expected for an assembly of pores having either a regular or irregular (nonconstant) section. These predictions over the scanning behavior within capillary condensation hysteresis can be used to check whether real materials are made up of independent pores or not. Our results are discussed in the light of experiments and density functional theory calculations for adsorption in porous media.

DOI: 10.1103/PhysRevB.72.024304 PACS number(s): 64.60.−i, 05.70.−a, 75.10.−b

I. INTRODUCTION

Adsorption isotherms in mesoporous materials (pore size in the range ~2–10 nm) usually exhibit a sharp increase of the adsorbed amount at a pressure below the bulk saturation pressure of the fluid. Such an increase corresponds to the capillary condensation of the fluid confined within the porous solid. In most systems, this phenomenon is accompanied with a large and reproducible hysteresis loop.[1–3] Experimental hysteresis loops are either symmetrical with quasiparallel adsorption/desorption branches (type $H1$) or asymmetrical with a desorption branch much steeper than the adsorption branch (type $H2$).[4] It is generally believed that the shape of the hysteresis loop is related to the absence or presence of connected pores in the porous material. The following International Union of Pure and Applied Chemists (IUPAC) classification has been proposed.[4] Type $H1$ hysteresis is usually interpreted as the signature of a material made up of unconnected pores. In this case, theoretical works based on density functional theory (DFT),[5,6] lattice gas models,[7] as well as molecular simulations[8,9] suggest that the hysteresis loop is a van der Waals loop of the confined system, i.e., an intrinsic property of the confined fluid. Such an interpretation is usually invoked to explain symmetrical hysteresis loops that are observed for MCM-41 and SBA-15 silica mesoporous materials.[10–15] On the other hand, a type $H2$ hysteresis loop is usually interpreted as experimental evidence of a material made up of connected pores, such as controlled pore glass and Vycor.[16–20] In this case, the irreversibility of the capillary condensation is often explained in terms of pore blocking effects, as proposed by Everett.[21] the pore filling occurs at a pressure related to the pore size whereas the liquid can only evaporate when the constriction, which isolates the pore from the gas, empties.[5,22,23]

It is found that, for most experimental systems, connected and unconnected porous materials lead to $H1$ and $H2$ capillary hysteresis loops, respectively. In the case of unconnected silica MCM-41 pores,[24] the hysteresis loops exhibit $H1$ hysteresis loops (see, for instance, Refs. 12–14). In the case of connected materials such as cagelike materials (FDU-1[25–27] or SBA-16[25]) and porous glasses,[16–20] adsorption hysteresis loops are of type $H2$ as expected from the IUPAC classification. However, there are a number of situations where the above correspondence between the shape of the hysteresis loop and the nature of the porous network is not valid. For instance, adsorption experiments for unconnected pores in porous silicon show that, despite the lack of interconnections between pores, the capillary condensation hysteresis is of type $H2$.[28–30] Moreover, recent simulation[31–35] and theoretical[35,36] works have shown that, even for a single pore, $H2$ hysteresis loops can be observed, provided that the pore size is inhomogeneous along the pore axis. In this case, the asymmetry of the hysteresis loop arises from pore blocking or cavitation effects that occur because of the constrictions inside the pore.

The situations described in the previous paragraph are examples where the correspondence between connected/unconnected pores and $H1/H2$ hysteresis loops fails in accounting for experimental observations. A simple analysis of the shape of the hysteresis loop does not provide reliable information about the topology of the porous material. In fact, the morphology (shape of the pores) as well as the topology of the porous network must be considered to obtain a clear picture of the hysteretic behavior of the capillary condensation phenomenon.[33,34] Powerful experiments to obtain insights into the nature of the hysteresis loop consist of measuring adsorption and desorption scanning curves as well as subloops. Adsorption (desorption) scanning curves are obtained by reversing upon desorption (adsorption) the direction of change in the pressure, while subloops consist of performing adsorption/desorption cycles within the main capillary condensation hysteresis loops. The independent domain theory developed by Everett[37–40] provides a framework for modeling scanning curves and subloops in capillary condensation hysteresis. This theory is an adaptation of the Preisach model that was developed to explain hysteretic magnetization in magnetic materials.[41] In the independent domain theory, it is assumed that the porous network can be de-

scribed as an assembly of domains that behave in an independent way upon adsorption and desorption. On this assumption, Everett established several theoretical predictions regarding the behavior of scanning curves and subloops of adsorption/desorption cycles in porous media. These predictions provide a set of tests to be used as a checking procedure to determine whether a porous material is made of independent pores or not.[39,40] However, as first noted by Enderby,[42,43] Everett neglects in the original formulation of the independent domain theory the existence of a molecularly thin film adsorbed on the pore surface prior to capillary condensation, i.e., in Everett's approach a domain is either completely empty or filled with the liquid. In the case of mesoporous systems (characteristic size about 2–10 nm), this approximation breaks down as the volume of the adsorbed film becomes comparable to the volume of the filled pore.[44]

The aim of this paper is to extend the domain theory proposed by Everett in order to account for the existence of the film adsorbed at the surface of the porous material. Following the previous work by Enderby,[42,43] we discuss how this affects the original predictions by Everett and establish a set of tests to check whether or not a porous material can be described as an assembly of independent domains. We consider the behavior of the scanning curves and subloops that is expected for (i) an assembly of independent pores and (ii) inhomogeneous pores (such as a pore with constrictions) or a network of connected pores. In both cases, we perform simulations based on the domain theory and compare the predictions with recent experiments[17,45–48] and density functional theory calculations[47,49] of adsorption in porous media. The remainder of the paper is organized as follows. In Sec. II, we extend the independent domain theory developed by Everett in order to take into account the presence of the film adsorbed at the surface of the pores. In Sec. III, we examine the predictions for the simple cases of an assembly of regular cylindrical pores and an assembly of constricted pores. In Sec. IV, we summarize and discuss our findings in the light of experimental and theoretical results for adsorption in porous materials.

II. INDEPENDENT DOMAIN THEORY

A. Everett's model

The independent domain theory developed by Everett allows one to describe the hysteretic adsorption/desorption behavior of a collection of independent pores. Let us divide the porous space of a solid into an assembly of domains; each domain is filled upon adsorption at a pressure x_{12} and emptied upon desorption at a pressure x_{21}. In the independent domain theory, it is assumed that each domain behaves as an independent system, i.e., as an isolated pore that is directly in contact with the external gas reservoir. Because pore condensation cannot occur at a pressure lower than the evaporation, each set (x_{12},x_{21}) must obey:

$$x_{12} \geqslant x_{21}. \tag{1}$$

We note that $x_{12}=x_{21}$ corresponds to a domain where capillary condensation is reversible. As shown in Fig. 1, the filling and emptying of the porous material can be described by reporting in a "complexion diagram" x_{21} as a function of x_{12}. Equation (1) implies that only the lower triangular part of the complexion diagram, i.e., below the diagonal $x_{12}=x_{21}$, represents porous domains.

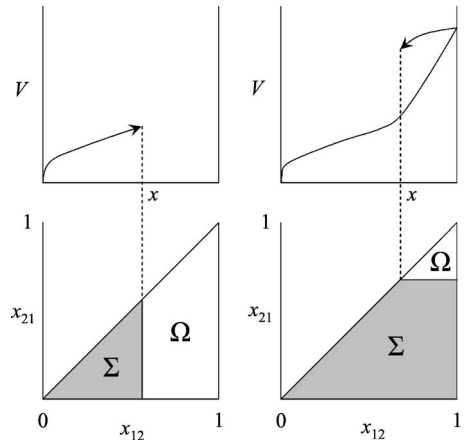

FIG. 1. (bottom) Complexion diagram for capillary condensation/evaporation in a porous material. Upon the adsorption process (left) porous domains $\mathbf{\Sigma}$ with $x_{12} \leqslant x$ are filled at a pressure x. Upon the desorption process (right) porous domains $\mathbf{\Omega}$ with $x_{21} > x$ are emptied at a pressure x. (top) Adsorption/desorption isotherms corresponding to each complexion diagram. Adapted from Everett (Ref. 40).

Upon the adsorption process, porous domains with $x_{12} \leqslant x$ are filled by the liquid at a pressure x (see Fig. 1). On the other hand, porous domains with $x_{21} > x$ are emptied at a pressure x upon the desorption process. At each surface element $dx_{12}dx_{21}$ of the complexion diagram, we define the function $v(x_{12},x_{21})$ such as that $v(x_{12},x_{21})dx_{12}dx_{21}$ is the volume of liquid in the porous domains in which (i) condensation occurs between x_{12} and $x_{12}+dx_{12}$ and (ii) evaporation occurs between x_{21} and $x_{21}+dx_{21}$. No assumption is made in what follows regarding the dependence of $v(x_{12},x_{21})$ on x_{12} and x_{21}, i.e., $v(x_{12},x_{21})$ is an arbitrary and independent function of its variables x_{12} and x_{21}. We also introduce the ensembles $\mathbf{\Sigma}$ and $\mathbf{\Omega}$ which correspond to the porous domains that are filled and emptied, respectively (note that these ensembles depend on the pressure x). The adsorbed amount $V(x)$ at a pressure x can be written in the general form:

$$V(x) = \int \int_{\mathbf{\Sigma}} dx_{12}dx_{21}v(x_{12},x_{21}). \tag{2}$$

Complexion diagrams are very convenient to describe any path followed by the system, including hysteresis loops, scanning curves, and subloops. For instance, let us consider a porous material partially filled by the liquid; one can sample the inside of the hysteretic region by reversing the direction of change in the pressure upon adsorption. The complexion diagram corresponding to such a desorption scanning curve is illustrated in Fig. 2. We also report in Fig. 2 the complexion diagram corresponding to an adsorption scanning curve, which is obtained by increasing the pressure starting from the desorption branch of the hysteresis loop.

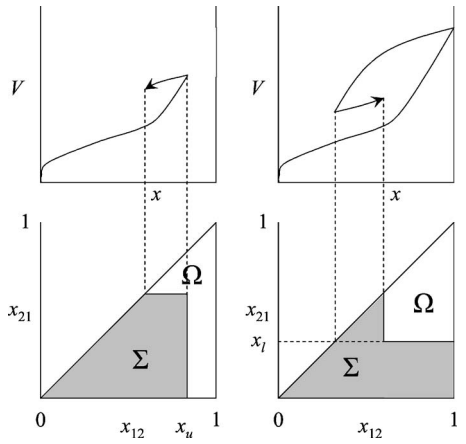

FIG. 2. (bottom) Complexion diagram for adsorption and desorption scanning curves in capillary condensation hysteresis. (top) Adsorption/desorption isotherms corresponding to each complexion diagram. Adapted from Everett (Ref. 40). The desorption scanning curve (left) is obtained by decreasing the pressure on the adsorption branch of the hysteresis loop. The adsorption scanning curve (right) is obtained by increasing the pressure on the desorption branch of the hysteresis loop. $\mathbf{\Sigma}$ and $\mathbf{\Omega}$ correspond to the porous domains that are filled and emptied, respectively.

On the basis of the formalism introduced above, Everett established a series of predictions for systems made of independent porous domains. The first theorem of Everett's theory states: if the descending scanning curves meet the desorption branch before the lowest closure point of the hysteresis loop, then the adsorption scanning curves will meet the adsorption branch before the highest closure point of the hysteresis loop. On the other hand, the second theorem predicts: if the descending scanning curves converge on the lowest closure point of the hysteresis loop, then the adsorption scanning curves will converge on the highest closure point of the hysteresis loop. The third theorem of the independent domain theory concerns the slope of the adsorption and desorption scanning curves (see Fig. 3). This theorem can be stated as follows: the slope $dV(x)/dx$ at x of a desorption scanning curve increases as its initial point x_u on the adsorption branch increases. Similarly, it can be shown that the slope $dV(x)/dx$ at x of an adsorption scanning curve decreases as its initial point x_l on the adsorption branch increases. Another important prediction that arises from the independent domain theory is the congruence of subloops (*fourth* theorem). Let us consider two adsorption/desorption cycles that are performed between the same lower x_l and upper x_u end point pressures, but different positions within the hysteresis loop (see Fig. 4). These two subloops are said to be congruent if they can be perfectly superimposed on the top of each other by a translation along the ordinate axis.[40,49]

The congruence property and the predictions over the behavior of the scanning curves are the main theorems that were established in the original independent domain theory. However, as already noted by Lilly and Hallock,[46] Everett neglected the existence of a film adsorbed at the surface of the porous domain, i.e., the adsorbed volume prior to capillary condensation ($x<x_{12}$) is 0. We previously mentioned that this assumption is not valid for mesoporous solids, as the

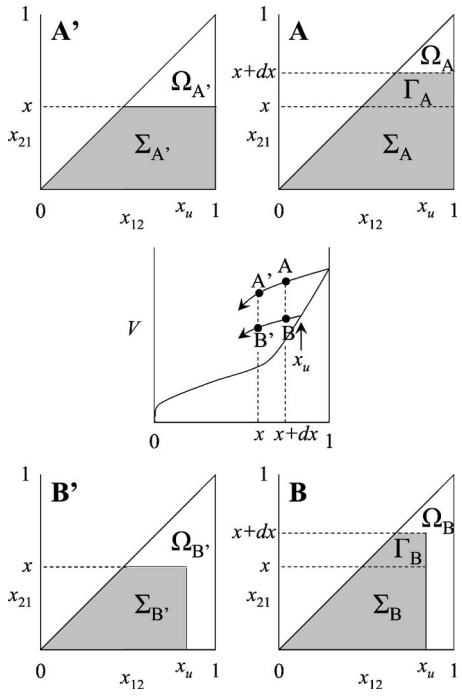

FIG. 3. (middle) Desorption curves originating from the adsorption branch of the hysteresis loop. x_u is the pressure at which the direction of change in pressure is reversed to obtain the desorption scanning curve containing the segment BB'. The points A, B and A', B' are located at a pressure $x+dx$ and x, respectively. (top) and (bottom) are the complexion diagrams corresponding to A, A', B and B'. $\mathbf{\Sigma}$ and $\mathbf{\Omega}$ correspond to the porous domains that are filled and emptied, respectively. $\mathbf{\Gamma_A}$ and $\mathbf{\Gamma_B}$ are the domains that evaporate when the pressure decreases from $x+dx$ down to x.

volume corresponding to the adsorbed film becomes comparable to the total porous volume (see Ref. 44). The attempt by Enderby in 1955[42,43] to include the adsorbed film in the independent domain theory has not had a large impact in the field of adsorption and condensation in porous media. As a result, experiments in the literature are still analyzed on the basis of Everett's original predictions.[45–49] In the following section, we extend the independent domain theory in order to account for the presence of the adsorbed film, using a very simple formalism. We show how the original predictions must be modified. We then discuss our results in the light of experiments and density functional theory calculations for adsorption in model porous media, which were not available when the original versions of the independent domain theory were developed.

B. Extended domain theory: Effect of the adsorbed film

In order to develop a domain theory that accounts for the film adsorbed at the pore surface, we use the formalism of the complexion diagrams described in the previous section. We introduce the function $w(x,x_{12},x_{21})$ that represents the adsorbed amount prior to capillary condensation. $w(x,x_{12},x_{21})$ is the adsorbed amount at a pressure x in porous domains for which (i) condensation occurs between x_{12} and $x_{12}+dx_{12}$ and (ii) evaporation occurs between x_{21} and x_{21}

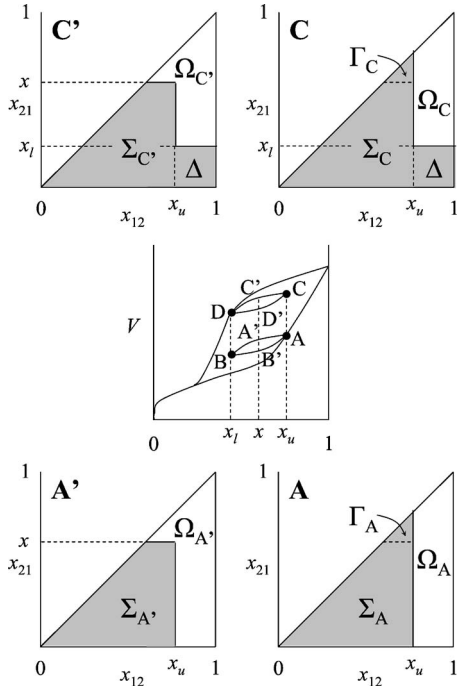

FIG. 4. (middle) Subloops (ABA) and (DCD) originating from the adsorption and desorption branches of the hysteresis loop, respectively. The two subloops are performed between the same lower x_l and upper x_u end-point pressures, but different positions within the hysteresis loop. The points A' and C' are located at a pressure x on the descending segment of the subloop (ABA) and (DCD), respectively. Similarly, the points B' and D' are located at a pressure x on the ascending segment of the subloop (ABA) and (DCD), respectively. (top) and (bottom) are the complexion diagrams corresponding to A, A', C, and C'. $\boldsymbol{\Sigma}$ and $\boldsymbol{\Omega}$ correspond to the porous domains that are filled and emptied, respectively. $\boldsymbol{\Gamma}_\mathbf{A}$ and $\boldsymbol{\Gamma}_\mathbf{C}$ are the domains that evaporate when the pressure decreases from x_u (A,C) down to x (A',C'). $\boldsymbol{\Delta}$ corresponds to the filled domains that are responsible for the difference in adsorbed amount between C (or C') and A (or A').

$+dx_{21}$. While $v(x_{12},x_{21})$ is assumed to be independent of the pressure (incompressible liquid), $w(x,x_{12},x_{21})$ is pressure dependent as the thickness of the adsorbed film increases with pressure (see, for instance, Refs. 50 and 51). Using the ensembles $\boldsymbol{\Sigma}$ and $\boldsymbol{\Omega}$ that we introduced previously (see Fig. 1), the adsorbed amount $V(x)$ upon adsorption and desorption can be written as

$$V(x) = \int\int_{\boldsymbol{\Sigma}} dx_{12}dx_{21}v(x_{12},x_{21}) + \int\int_{\boldsymbol{\Omega}} dx_{12}dx_{21}w(x,x_{12},x_{21}). \tag{3}$$

The first term represents the condensed volume and is, of course, identical to that given by Eq. (2). The second term in Eq. (3) represents the adsorbed volume that is due to porous domains that are not filled by the liquid.

In order to discuss the validity of the *third* theorem of Everett's theory, we first consider two desorption scanning curves that originate from the main adsorption branch of the hysteresis loop (see Fig. 3). The points A, B and A', B' are located at a pressure $x+dx$ and x, respectively. Complexion diagrams corresponding to A, A', B, and B' are also reported in Fig. 3. The change in the adsorbed amount when the system goes from A to A' is

$$\begin{aligned} dV_{A'} = V_A - V_{A'} = &\int\int_{\boldsymbol{\Sigma}_\mathbf{A}} dx_{12}dx_{21}v(x_{12},x_{21}) \\ &+ \int\int_{\boldsymbol{\Omega}_\mathbf{A}} dx_{12}dx_{21}w(x+dx,x_{12},x_{21}) \\ &- \int\int_{\boldsymbol{\Sigma}_{\mathbf{A}'}} dx_{12}dx_{21}v(x_{12},x_{21}) \\ &- \int\int_{\boldsymbol{\Omega}_{\mathbf{A}'}} dx_{12}dx_{21}w(x,x_{12},x_{21}). \end{aligned} \tag{4}$$

It is convenient to rewrite Eq. (4) as

$$\begin{aligned} dV_{A'} = V_A - V_{A'} = &\int\int_{\Gamma_A} dx_{12}dx_{21}\{v(x_{12},x_{21}) - w(x,x_{12},x_{21})\} \\ &+ \int\int_{\boldsymbol{\Omega}_A} dx_{12}dx_{21}\{w(x+dx,x_{12},x_{21}) - w(x,x_{12},x_{21})\}, \end{aligned} \tag{5}$$

where $\boldsymbol{\Gamma}_\mathbf{A}$ is the assembly of domains that evaporate when the pressure decreases from $x+dx$ down to x. The first integral in Eq. (5) corresponds to the domains that are filled in A and empty in A' (i.e., domains $\boldsymbol{\Gamma}_\mathbf{A}$). The second integral in Eq. (5) accounts for the decrease of the film thickness in pores that were already empty in A (i.e., domains $\boldsymbol{\Omega}_\mathbf{A}$). Similarly, the change in the adsorbed amount when the system goes from B to B' can be written as

$$\begin{aligned} dV_{B'} = V_B - V_{B'} = &\int\int_{\Gamma_B} dx_{12}dx_{21}\{v(x_{12},x_{21}) - w(x,x_{12},x_{21})\} \\ &+ \int\int_{\boldsymbol{\Omega}_B} dx_{12}dx_{21}\{w(x+dx,x_{12},x_{21}) - w(x,x_{12},x_{21})\}. \end{aligned} \tag{6}$$

The slopes at x of the desorption scanning curves can be evaluated from Eqs. (5) and (6), provided A' and B' tend to A and B ($dx \sim 0$). For all x, these derivatives $dV_{A'}/dx$ and $dV_{B'}/dx$ are necessarily positive since (i) the total adsorbed amount $v(x_{12},x_{21})$ is larger than the volume corresponding to the adsorbed film $w(x,x_{12},x_{21})$ and (ii) the adsorbed amount $w(x,x_{12},x_{21})$ increases when the pressure increases from x to $x+dx$. Given that Γ_B is included in Γ_A, the first term in Eq. (6) is smaller than that for Eq. (5). On the other hand, Ω_B includes Ω_A so that the second term in Eq. (6) is larger than that for Eq. (5). The last two inequalities show that it is not possible, *a priori*, to determine which of the slopes $dV_{A'}/dx$ and $dV_{B'}/dx$ is the largest one. A similar conclusion is reached in the case of adsorption scanning curves. This result shows that the *third* theorem of the independent domain theory is not valid if the film adsorbed at the pore surface is taken into account.

We now examine the validity of the *fourth* theorem of the independent domain theory, regarding the congruence of subloops performed between the same end-point pressures x_l and x_u. Let us consider the case of the subloops $(AA'BB'A)$ and $(DD'CC'D)$ shown in Fig. 4. A convenient definition of the congruence property is as follows. Two subloops are congruent if the change in the adsorbed amount when the pressure varies from the end point to x is the same for the two subloops. Of course, the previous property must be verified for both the ascending and descending segments of the subloops. Using the set of points defined in Fig. 4 (A,A',B,B',C,C',D,D'), the congruence property can be expressed as

$$\left.\begin{aligned} V_A - V_{A'} &= V_C - V_{C'} \\ V_B - V_{B'} &= V_D - V_{D'} \end{aligned}\right\} \forall\, x \in [x_l, x_u]. \tag{7}$$

Let $dV_{A'}=V_A-V_{A'}$ and $dV_{C'}=V_C-V_{C'}$ be the change in adsorbed amount between A' and A and between C' and C, respectively. As can be seen in Fig. 4, the difference between $dV_{A'}$ and $dV_{C'}$ corresponds to the variation of the adsorbed film at the surface of porous domains $\mathbf{\Delta}$, which are filled in C (or C') but emptied in A (or A'):

$$dV_{A'} - dV_{C'} = \int\int_{\mathbf{\Delta}} dx_{12}dx_{21}\{w(x+dx,x_{12},x_{21}) - w(x,x_{12},x_{21})\}. \tag{8}$$

It can be easily derived that the difference between $dV_{B'}=V_B-V_{B'}$ and $dV_{D'}=V_D-V_{D'}$ is similar to Eq. (8). Given that $w(x,x_{12},x_{21})$ is an increasing function of the pressure x, Eq. (8) shows that the difference of slopes between the segment AA' and CC' is positive, i.e., $dV_{A'}/dx > dV_{C'}/dx\ \forall x \in [x_l,x_u]$. This further shows that two subloops performed between the same end points cannot be congruent; the *fourth* theorem of the independent domain theory is not valid, unless (i) the adsorbed film is neglected, i.e., $w(x,x_{12},x_{21})=0\ \forall x$, or (ii) its thickness is assumed to be independent of the pressure, i.e., $w(x,x_{12},x_{21})=\text{const}\ \forall x$. This effect due to the variation of the film thickness must explain, at least partly, the lack of congruence that has been observed in many experiments.[45–47] However, as will be discussed below, the noncongruence of subloops in the case of connected porous materials is also expected because of the nonindependence of the pores, i.e., in addition to the effect of the adsorbed film.

III. RESULTS

A. Method

It has been seen in the previous section that the *third* and *fourth* theorems of the independent domain theory are not valid if the existence of the film adsorbed at the pore surface is taken into account. In the theory proposed by Everett[40] and Enderby,[42,43] x_{12} and x_{21} are not correlated except through the inequality (1). It appears that this situation is too general since both the capillary condensation and evaporation pressures are related to the size of the pore (we recall that x_{12} and x_{21} are the filling and emptying pressures when the domain is taken as an isolated pore directly in contact with the external gas reservoir). In what follows, we restrict ourselves to the case where both the condensation and evaporation pressures (x_{12}^k, x_{21}^k) for a porous domain k are an increasing function of its size r_k: $r_{k1} > r_{k2} \Leftrightarrow x_{12}^{k1} > x_{12}^{k2}$ and $x_{21}^{k1} > x_{21}^{k2}$. We note that in this case the couples (x_{12}^k, x_{21}^k) correspond to a line instead of a cloud of points in the complexion diagram (x_{12},x_{21}).

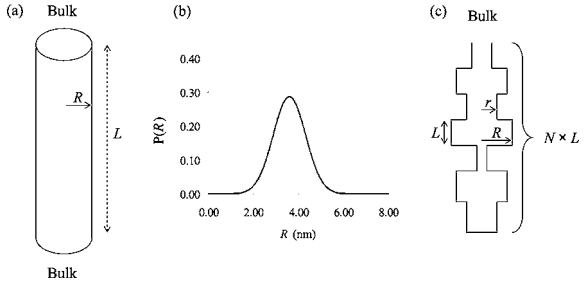

FIG. 5. (a) Schematic view of model A: each pore of radius R and length L is independent and is in direct contact with the bulk external reservoir. (b) The pore size distribution used for the assembly of independent cylindrical pores is a Gaussian distribution. The average pore radius is 3.6 nm and the dispersion 0.72 nm (given by the σ of the Gaussian function). (c) Schematic view of the pore with constrictions, i.e., model B: each pore is modeled as an assembly of N alternating cavities and constrictions of the same length L (in this example, $N=7$). Each constricted pore of length $N\times L$ is in contact with the bulk external reservoir through its first constriction. The cavity and constriction sizes are chosen randomly in the ranges $4.2+/-0.5$ nm and $3.6+/-0.5$ nm, respectively.

In this work, we calculated the N_2 adsorption/desorption isotherms, scanning curves and subloops at 77 K for two different models (A, B) of porous materials. Model A is an assembly of independent pores k having a regular cylindrical section R_k and the same length L; each pore is an independent domain in this case. The pore radius distribution R_k is a Gaussian function centered about $R_0=3.6$ nm with $\sigma=0.72$ nm [see Fig. 5(a)]; the same pore size distribution was used by Ball and Evans in their previous study on the temperature dependence of adsorption in mesoporous materials.[5] For this model, each pore of radius R_k and length L is an independent porous domain k that corresponds to a total volume of $\pi L R_k^2$. x_{12}^k (x_{21}^k) was related to the pore size R_k using the modified Kelvin equation[3,52] and assuming that the gas/liquid interface inside the pore forms a cylindrical (hemispherical) meniscus.[6,29,53–56] The thickness of the adsorbed film, $t(x)$, at a pressure x was estimated using an empirical equation of the type Harkins–Jura[1,2] with the parameters proposed by Kruk and co-workers.[10,11] The total adsorbed amount $V(x)$ at a pressure x upon adsorption or desorption is easily computed using Eq. (3) with the following relations: $v(x_{12}^k,x_{21}^k)=N(R_k)\times\pi L R_k^2$ and $w(x,x_{12}^k,x_{21}^k)=N(R_k)\times\pi L\{R_k^2-[R_k-t(x)]^2\}$, where $N(R_k)$ is the number of pores of radius R_k. As previously mentioned in Sec. II B, it is assumed in these calculations that $v(x_{12}^k,x_{21}^k)$ is independent of the pressure (incompressible liquid), while $w(x,x_{12}^k,x_{21}^k)$ is pressure dependent as the thickness of the adsorbed film increases with pressure. It is worth mentioning that the inaccuracy of

the Kelvin equation in predicting the experimental transition pressures is not of fundamental importance in this work since we are mainly interested in the qualitative behavior of the scanning curves and subloops for connected/unconnected porous materials. An estimate of the condensation/evaporation pressures from molecular simulations would lead to a similar behavior to that observed with the modified Kelvin equation (we note that the latter equation used with bulk parameters for the surface tension and density has been shown to break down for pore sizes smaller than 16 molecular diameters, approximately[3]).

Model B is an assembly of cylindrical pores made of N alternating cavities and constrictions of the same length $L=1$ nm intervals [see Fig. 5(c)]. Cavities and constrictions in this system are nonindependent domains as the condensation and evaporation pressures are influenced by the neighbor domains (see below). The cavity and constriction sizes are chosen randomly in the ranges $4.2+/-0.5$ nm and $3.0+/-0.5$ nm, respectively. The global average pore size (cavity +construction) is 3.6 nm as for model A. Each of these constricted pores of length $N\times L$ is in contact with the bulk phase through its first constriction. Model B mimics a collection of cylindrical pores having a nonuniform pore size distribution; however, inhomogeneities in the condensation or evaporation pressures along the pore axis can be caused by other factors, such as the existence of chemical defects at the pore surface. For instance, Bock *et al.* have shown that such a chemical heterogeneity leads to a very complex phase diagram of the confined fluid, even though the pore size is constant.[57,58]

Following the previous work by Cordero *et al.*,[59] the adsorbed volume for model B was calculated as follows. Upon adsorption, a porous domain k is filled if one of the following conditions is fulfilled: (a) if its two neighbors $k+1$ and $k-1$ are empty, then k of smaller diameter will be filled at a pressure given by the modified Kelvin equation with a cylindrical meniscus; and (b) if $k+1$ or $k-1$ is filled, then k will be filled when the hemispherical meniscus at the opening between $k+1$ and k or $k-1$ and k can propagate into the empty cavity k. The latter condition, called advanced condensation[48] or pore assisting factor,[59] occurs when x reaches the pressure given by the modified Kelvin equation with a hemispherical meniscus. Upon desorption, k is emptied according to one of the following processes. (a) If $k+1$ or $k-1$ are empty, then k is in contact with the gas phase and emptying will occur when the hemispherical meniscus between k and its emptied neighbor can recess through k. (b) If $k+1$ and $k-1$ are filled, then k will not empty until either $k+1$ or $k-1$ evaporates. The latter process corresponds to the well-known pore blocking effect introduced by Everett.[21] We emphasize that the adsorbed film is also taken into account in model B, using the Harkins–Jura equation (as in the case of model A). Model B departs from the model developed by Mason to account for scanning loops observed in disordered porous materials.[22,23] First of all, Mason's model does not include the cooperative effect due to advanced condensation but only that due to pore blocking. In contrast to model B, Mason assumed that filling and emptying pressures are identical so that condensation in a single, isolated domain is reversible. Finally, Mason's theory does not include pore blocking effects for cylindrical pores because of restrictive conditions on the hierarchy of cavity and constriction sizes (for details, see discussion in Ref. 5). More recently, Guyer and McCall[60] considered condensation and evaporation in a two-dimensional network of connected cylindrical pores. However, the authors do not account for the existence of the adsorbed film so that their model is similar to that proposed by Everett in his attempt to describe interacting pores.[21]

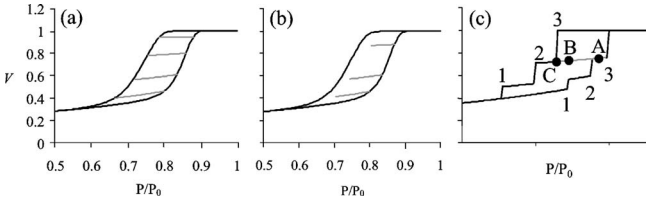

FIG. 6. (a) Desorption scanning curves and (b) subloops for N_2 at 77 K in an assembly of independent cylindrical pores of various diameters. The pore size distribution is a Gaussian function centered about $R_0=3.6$ nm with $\sigma=0.72$ nm (model A). (c) Schematic adsorption/desorption isotherm for a set of three independent cylindrical pores. The numbers 1, 2, 3 on the adsorption (desorption) branch indicate the condensation (evaporation) pressure for each pore. AC is a desorption scanning curve starting from a configuration where 3 is empty while 1 and 2 are filled. The point B is located on the segment AC at a pressure larger than the desorption branch.

B. Regular cylindrical pores

The adsorption isotherm as well as scanning curves for model A are shown in Fig. 6(a). In agreement with the previous work by Cordero *et al.*, the desorption scanning curves meet the desorption branch at a pressure above the lowest closure point of the hysteresis loop. We also found that the adsorption scanning curves meet the adsorption branch at a pressure below the highest closure point of the hysteresis loop. The interpretation of such a behavior can be easily understood by considering in Fig. 6(c) the schematic adsorption isotherm for a set of three independent cylindrical pores such as $r_1<r_2<r_3$. We have also reported the desorption scanning curve that originates from A where 3 is empty while 1 and 2 are filled. Clearly, the descending curve starting from A will meet the desorption branch in C, since evaporation of 1 and 2 cannot occur before the pressure x decreases down to x_{21}^1 and x_{21}^2, respectively. Let us now consider the following experimental process: when the scanning curve starting from A reaches B, the direction of change in the pressure is reversed so that the system evolves back to A. This thermodynamic path must be reversible since the variation in the adsorbed amount along AB is only due to the decrease of the thickness of the film adsorbed in 3 (1 and 2 are not involved in this process since they remain filled by the liquid at all pressures between A and B). In agreement with this prediction, we found that the adsorption/desorption cycles performed within the main hysteresis loop are perfectly reversible for model A [see Fig. 6(b)].

C. Cylindrical pore with constrictions

We now discuss the scanning curves and subloops obtained for model B, i.e., a cylindrical pore having a noncon-

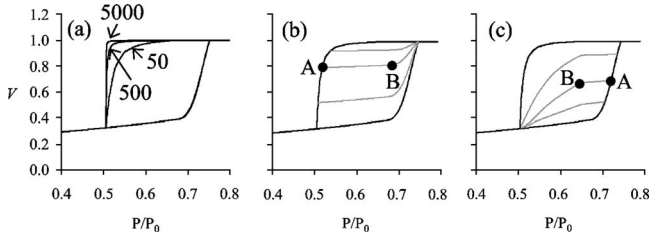

FIG. 7. (a) N_2 adsorption isotherm at 77 K for cylindrical pores having a nonconstant diameter along their revolution axis; each pore is an alternating sequence of N cavities and constrictions (model B). The average cavity and constriction sizes are 4.2 and 3.0 nm, respectively (see text). Each desorption curve corresponds to a different number N as indicated in the graph. (b) Adsorption and (c) desorption scanning curves obtained for model B with $N=100$.

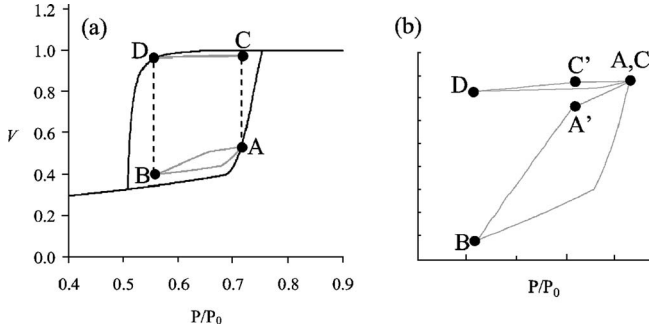

FIG. 8. (a) Subloops (*ABA*) and (*DCD*) originating from the adsorption and desorption branches of the hysteresis loop obtained for N_2 at 77 K in model B with $N=100$. The two subloops are performed between the same pressures $P/P_0=0.56$ and 0.72, but different positions within the hysteresis loop. (b) Comparison of the subloops shown in (a); the right end point C of the subloop (*DCD*) has been shifted to overlap with A.

stant section along its pore axis. All the calculations have been averaged over 500 realizations in order to obtain significant results that are not sample dependent. The adsorption/desorption isotherm for model B is shown in Fig. 7(a) for different numbers N of constrictions and cavities. Interestingly, the desorption becomes steeper as N increases, while the adsorption remains unaffected by a change in N. This effect of the pore length N on the desorption branch can be understood as follows. Except for cavities located in the vicinity of the bulk phase, i.e., nonblocked cavities, the emptying mechanism is triggered by the evaporation of the closest constriction to the pore opening. When the pore length increases, the fraction of pores that are blocked by the constriction close to the bulk increases and, consequently, the desorption branch appears steeper. In contrast, the condensation mechanism is not governed by the interfacial region between the pore opening and the bulk reservoir so that the adsorption branch is not sensitive to the pore length N.

Adsorption and desorption scanning curves for model B with $N=100$ are shown in Figs. 7(b) and 7(c), respectively (we checked that the qualitative behavior of these curves does not depend on the pore length). In contrast to model A, the adsorption and desorption scanning curves for model B meet the hysteresis loop at its closure point. We note that, in agreement with the experiments by Brown,[17] Mason's theory predicts a similar behavior to that in Fig. 7 in the case of connected porous materials where each cavity is isolated from the rest of the porosity by several constrictions[5,61] (see also Ref. 59 for a complete study of the effect of the number of connections on the scanning curves). Each adsorption (desorption) scanning curve first exhibits a nearly flat portion *AB* until it increases (decreases) sharply toward the closure point of the hysteresis loop. This plateau corresponds to a range of pressure where no pore filling or emptying occurs, but only a change in the thickness of the adsorbed film.

We now consider in Fig. 8(a) two subloops *ABA* and *DCD* obtained between the same end-point pressure $x=0.56$ and 0.72. Clearly, the two subloops have different shapes and, therefore, are not congruent [see Fig. 8(b) where the right end point C of the subloop *DCD* has been shifted to overlap with A]. As in the case of the scanning curves in Fig. 7, the subloops *ABA* and *DCD* exhibit a nearly flat portion that corresponds to a range where variations in the adsorbed amount are only due to increase or decrease in the thickness of the adsorbed film. Even for this portion where no pore filling/emptying occurs, the slopes of the segments AA' and CC' are different. This result is an illustration of what has been concluded in Sec. II: two subloops cannot be congruent because of the film adsorbed at the pore surface. Of course, the noncongruence observed for model B is also related to the fact that cavities and constrictions do not behave independently upon adsorption and desorption.

IV. DISCUSSION AND CONCLUSION

In the first part of this work, we have discussed how Everett's domain theory must be modified in order to account for the presence of the film adsorbed at the pore surface. We have seen that the original predictions are not valid unless the existence of the adsorbed film is neglected or its thickness is assumed to be independent of the pressure. For instance, the lack of congruence of two subloops performed between the same lowest and highest pressures cannot be attributed only to the nonindependence of the porous domains, in contrast to what is usually written in the literature.[45–47,49] However, there are situations where the noncongruence of subloops can be attributed mainly to the fact that the porous domains interact with each other. For instance, anopore or nuclepore materials studied by Hallock and co-workers have very large pores, $D\sim 200$ nm, so that the volume corresponding to the adsorbed film can reasonably be neglected compared to the total pore volume.[45–47] Moreover, direct evidence for the nonindependence of the pores in these materials have also been reported.[45,46]

In the second part of this work, we investigated the case where both the capillary condensation and evaporation pressures are increasing functions of the domain size. We consider two different porous systems that are either made up of independent or dependent domains. Model A is an assembly of independent cylindrical pores having a constant section; each pore is an independent domain in this case. Model B is an assembly of cylindrical pores having a nonconstant sec-

tion so that each pore is made up of nonindependent domains. On this assumption, we have seen that an assembly of pores made up of independent (model A) and nonindependent (model B) domains must obey the following properties.

(a) Scanning curves for independent porous domains must meet the adsorption/desorption branch at a pressure different from the closure points of the hysteresis loop [see Fig. 6(a)]. In contrast, scanning curves for nonindependent systems (model B) must meet the hysteresis loop at its closure point [Figs. 7(b) and 7(c)].

(b) Scanning curves for an assembly of independent domains are necessarily reversible so that it is not possible to observe subloops within the main capillary hysteresis loop [Fig. 6(b)]. On the contrary, noncongruent subloops are observed for a collection of interacting domains; the noncongruence is due to the nonindependence of the domains, in addition to an effect of the variation in the adsorbed film at the pore surface (Fig. 8).

Properties (a) and (b) compose a set of tests that can be used to check whether pores of a material can be considered as an assembly of independent domains or not. For instance, a recent experimental investigation of N_2 adsorption in SBA-15 has shown that the scanning curves do not fulfill criterion (a) for independent systems, i.e., the adsorption (desorption) scanning curves meet the hysteresis at its highest (lowest) closure point. As proposed by Esparza *et al.* on the basis of density functional theory calculations, the experimental scanning behavior observed for SBA-15 materials suggests that the pores cannot be described as an assembly of independent porous domains, but rather as undulated pores (i.e., alternating cavities and constrictions as in model B).

The case of MCM-41 is more ambiguous; McNall *et al.* have shown that the shape of the scanning curves for this type of system depends on the size of the pores.[62] On the one hand, scanning curves for large pore diameters ($D \geqslant 3.6$ nm for N_2 or Ar) are converging, i.e., meet the hysteresis loop at its closure point. On the other hand, scanning curves for smaller pores are crossing, i.e., meet the hysteresis loop before its closure point. The nonindependent pores behavior observed for the large MCM-41 pores was first observed by Kruk and co-workers who only considered pores with $D > 4.6$ nm.[63] These last results suggest that large MCM-41 pores, unlike the small ones, exhibit size undulation along their axis (as in the case of SBA-15 materials), which explains the nonindependent pores behavior of the scanning curves. We note that such an explanation is supported by the scattering experiments reported by Sonwane *et al.*[64] Further experiment for MCM-41 and SBA-15 pores, including a test of the criterion (b), should confirm the previous conclusion.

In their experimental work, McNall *et al.* also reported that N_2 desorption scanning curves for the largest MCM-41 pores ($D=5.1$ nm) do not meet the desorption branch but rather meet the lowest part of the adsorption branch.[62] This type of behavior, referred to as "returning" in Ref. 62, cannot be explained in the framework of model A or B or any existing theory (Mason's model[23] or Cordero's model[59]). This result suggests that synthesis conditions may not have led to MCM-41 samples having the usual pore features, i.e., a regular cylindrical section having a constant radius. Further study is needed to clarify this issue.

In Sec. III, we also found that the desorption branch for nonindependent porous domains appears steeper as the size of the sample increases, while the adsorption remains unaffected. This property constitutes a test of whether pore blocking effects occur upon desorption. For instance, such a test could be used to clarify[28,29] or corroborate[30] recent experiments on desorption processes in noninterconnected porous silicon since the pores can be prepared of different lengths.[65] However, one of the limitations of the model B in this paper arises from the fact that we neglect a possible desorption mechanism by cavitation, i.e., spontaneous nucleation of a gas bubble within the porous material.[31,34] Indeed, recent theoretical[36] and experimental[25] studies of adsorption in cagelike porous materials[66–68] have shown that, depending on the cavity, constriction sizes, and temperature, it can be more favorable to empty the pore through a cavitation phenomenon than a pore blocking effect.

ACKNOWLEDGMENTS

It is a pleasure to thank Dr. Henry Bock and Dr. Martin-Luc Rosinberg for helpful discussions. B. C. and K. E. G. are grateful to the National Science Foundation (Grants No. CTS-0211792 and INT-0089696) and the Petroleum Research Fund of the American Chemical Society for funding of this work. This research was performed using supercomputing resources from the National Partnership for Advanced Computational Infrastructure (NSF/NRAC Grant No. MCA93SO11) and the National Energy Research Scientific Computing Center (DOE-DE-FGO2-98ER14847).

*Corresponding author. Present address: Laboratoire de Physicochimie de la Matière Condensée (CNRS-UMR 5617), Université de Montpellier II, Place Eugène Bataillon, 34095 Montpellier Cedex 5, France. Email address: bcoasne@lpmc.univ-montp2.fr

[1] S. J. Gregg and K. S. W. Sing, *Adsorption, Surface Area and Porosity* (Academic Press, London, 1982).

[2] F. Rouquerol, J. Rouquerol, and K. S. W. Sing, *Adsorption by Powders and Porous Solids* (Academic Press, London, 1999).

[3] L. D. Gelb, K. E. Gubbins, R. Radhakrishnan, and M. Sliwinska-Bartkowiak, Rep. Prog. Phys. **62**, 1573 (1999).

[4] K. S. W. Sing, D. H. Everett, R. A. Haul, L. Moscou, R. A. Pierotti, J. Rouquerol, and T. Siemieniewska, Pure Appl. Chem. **57**, 603 (1985).

[5] P. C. Ball and R. Evans, Langmuir **5**, 714 (1989).

[6] R. Evans, U. Marini Bettolo Marconi, and P. Tarazona, J. Chem. Soc., Faraday Trans. 2 **82**, 1763 (1986).

[7] R. Evans, J. Phys.: Condens. Matter **2**, 8989 (1990).

[8] J. P. R. B. Walton and N. Quirke, Mol. Simul. **2**, 361 (1989).

[9] G. S. Heffelfinger, F. Van Swol, and K. E. Gubbins, J. Chem. Phys. **89**, 5202 (1988).

[10] M. Kruk, M. Jaroniec, and A. Sayari, Langmuir **13**, 6267 (1997).
[11] M. Kruk, M. Jaroniec, C. H. Ko, and R. Ryoo, Chem. Mater. **12**, 1961 (2000).
[12] M. Kruk and M. Jaroniec, Chem. Mater. **12**, 222 (2000).
[13] K. Morishige, H. Fujii, M. Uga, and D. Kinukawa, Langmuir **13**, 3494 (1997).
[14] K. Morishige and M. Shikimi, J. Chem. Phys. **108**, 7821 (1998).
[15] K. Morishige and M. Ito, J. Chem. Phys. **117**, 8036 (2002).
[16] S. Nuttall, Ph.D. thesis, University of Bristol, 1974.
[17] A. J. Brown, Ph.D. thesis, University of Bristol, 1963.
[18] A. J. Brown, C. G. V. Burgess, D. H. Everett, and S. Nuttall, *Proceedings of the Characterization of Porous Solids Conference IV*, edited by B. McEnaney, F. Rodriguez-Teinoso, J. Rouquerol, K. S. W. Sing, and K. K. Unger (Elsevier, Amsterdam, 1997).
[19] S. Gross and G. H. Findenegg, Ber. Bunsenges. Phys. Chem. **101**, 1726 (1997).
[20] W. D. Machin, Langmuir **10**, 1235 (1994).
[21] D. H. Everett, in *The Structure and Properties of Porous Materials*, edited by D. H. Everett and F. S. Stone (Butterworths, London, 1958), p. 95; J. A. Barker, *ibid.*, p. 125.
[22] G. Mason, J. Colloid Interface Sci. **88**, 36 (1982).
[23] G. Mason, Proc. R. Soc. London, Ser. A **415**, 453 (1988).
[24] J. S. Beck, J. C. Vartulli, W. J. Roth, M. E. Leonowicz, C. T. Kresge, K. D. Schmitt, C. T.-W. Chu, D. H. Olson, E. W. Sheppard, S. B. McCullen, J. B. Higgins, and J. L. Schlenker, J. Am. Chem. Soc. **114**, 10834 (1992).
[25] P. I. Ravikovitch and A. V. Neimark, Langmuir **18**, 9830 (2002).
[26] M. Kruk, V. Antochshuk, J. R. Matos, L. P. Mercuri, and M. Jaroniec, J. Am. Chem. Soc. **124**, 768 (2003).
[27] M. Kruk and M. Jaroniec, Chem. Mater. **15**, 2942 (2003).
[28] B. Coasne, A. Grosman, N. Dupont-Pavlovsky, C. Ortega, and M. Simon, Phys. Chem. Chem. Phys. **3**, 1196 (2001).
[29] B. Coasne, A. Grosman, C. Ortega, and M. Simon, Phys. Rev. Lett. **88**, 256102 (2002).
[30] D. Wallacher, N. Kunzner, D. Kovalev, N. Knorr, and K. Knorr, Phys. Rev. Lett. **92**, 195704 (2004).
[31] L. Sarkisov and P. A. Monson, Langmuir **17**, 7600 (2001).
[32] A. Vishnyakov and A. V. Neimark, Langmuir **19**, 3240 (2003).
[33] B. Coasne and R. J.-M. Pellenq, J. Chem. Phys. **121**, 3767 (2004).
[34] B. Coasne, K. E. Gubbins, and R. J.-M. Pellenq, Part. Part. Syst. Charact. **21**, 149 (2004).
[35] B. Libby and P. A. Monson, Langmuir **20**, 4289 (2004).
[36] P. I. Ravikovitch and A. V. Neimark, Langmuir **18**, 1550 (2002).
[37] D. H. Everett and W. I. Whitton, Trans. Faraday Soc. **48**, 749 (1952).
[38] D. H. Everett and F. W. Smith, Trans. Faraday Soc. **50**, 187 (1954).
[39] D. H. Everett, Trans. Faraday Soc. **50**, 1077 (1954).
[40] D. H. Everett, in *The Solid-Gas Interface*, Vol. 2, edited by E. A. Flood (Marcel Dekker, New York, 1967), pp. 1055–1113.
[41] F. Preisach, Z. Phys. **94**, 277 (1935).
[42] J. A. Enderby, Trans. Faraday Soc. **51**, 835 (1955).
[43] J. A. Enderby, Trans. Faraday Soc. **52**, 106 (1956).
[44] Let us consider a 1σ thick film adsorbed at the surface of a cylindrical pore of radius $R=5\sigma$ (σ is the size of the adsorbed molecule). The volume corresponding to the adsorbed film is 36% of the total pore volume. Moreover, we expect the film thickness to be larger than 1σ since multilayer adsorption is usually observed for mesoporous materials (see, for instance, Refs. 50 and 51).
[45] M. P. Lilly, P. T. Finley, and R. B. Hallock, Phys. Rev. Lett. **71**, 4186 (1993).
[46] M. P. Lilly and R. B. Hallock, Phys. Rev. B **63**, 174503 (2001).
[47] A. H. Wooters and R. B. Hallock, J. Low Temp. Phys. **121**, 549 (2000).
[48] J. M. Esparza, M. L. Ojeda, A. Campero, A. Dominguez, I. Kornhauser, F. Rojas, A. M. Vidales, R. H. Lopez, and G. Zgrablich, Colloids Surf., A **241**, 35 (2004).
[49] E. Kierlik, P. A. Monson, M. L. Rosinberg, and G. Tarjus, J. Phys.: Condens. Matter **14**, 9295 (2002).
[50] B. Coasne, A. Grosman, C. Ortega, and R. J.-M. Pellenq, *Studies in Surface Science and Catalysis*, edited by F. Rodriguez-Reinoso, B. McEnaney, J. Rouquerol, and K. K. Unger (Elsevier Science, New York, 2002), Vol. 144, pp. 35–42.
[51] B. Coasne and R. J.-M. Pellenq, J. Chem. Phys. **120**, 2913 (2004).
[52] M. Kruk, M. Jaroniec, Y. Sakamoto, O. Terasaki, R. Ryoo, and C. H. Ko, J. Phys. Chem. B **104**, 292 (2000).
[53] M. W. Cole and W. F. Saam, Phys. Rev. Lett. **32**, 985 (1974).
[54] W. F. Saam and M. W. Cole, Phys. Rev. B **11**, 1086 (1975).
[55] L. H. Cohan, J. Am. Chem. Soc. **60**, 433 (1938).
[56] R. J. M. Pellenq and R. P. O. Denoyel, in *Fundamentals of Adsorption 7*, edited by K. Kaneko, H. Kanoh, and Y. Hanzawa (IK International, Chiba-City, 2002), p. 352.
[57] H. Bock and M. Schoen, Phys. Rev. E **59**, 4122 (1999).
[58] H. Bock, D. J. Diestler, and M. Schoen, J. Phys.: Condens. Matter **13**, 4697 (2001).
[59] S. Cordero, F. Rojas, I. Kornhauser, A. Dominguez, A. M. Vidales, R. Lopez, G. Zgrablich, and J. L. Riccardo, Appl. Surf. Sci. **196**, 224 (2002).
[60] R. A. Guyer and K. R. McCall, Phys. Rev. B **54**, 18 (1996).
[61] G. Mason, Proc. R. Soc. London, Ser. A **390**, 47 (1983).
[62] M. McNall, R. L. Laurence, and W. Curtis Conner, Microporous Mesoporous Mater. **44–45**, 709 (2001).
[63] M. Kruk, M. Jaroniec, and A. Sayari, Adsorption **6**, 47 (2000).
[64] C. G. Sonwane, S. K. Bhatia, and N. J. Calos, Langmuir **15**, 4603 (1999).
[65] O. Bisi, S. Ossicini, and L. Pavesi, Surf. Sci. Rep. **38**, 1 (2000).
[66] C. Yu, Y. Yu, L. Miao, and D. Zhao, Microporous Mesoporous Mater. **65**, 44 (2001).
[67] Y. H. Sakamoto, M. Kaneda, O. Terasaki, D. Y. Zhao, J. M. Kim, G. Stucky, H. J. Shim, and R. Ryoo, Nature (London) **408**, 449 (2000).
[68] P. Van Der Voort, M. Benjelloun, and E. F. Vansant, J. Phys. Chem. B **106**, 9027 (2002).